Neutron-multiplicity distributions for $(\alpha, xn\gamma)$ reactions with $E_\alpha = 50-120$ MeV and the pre-equilibrium neutron deexcitation processes

K. Maeda, * T. Shibata, and H. Ejiri

Department of Physics, Osaka University, Toyonaka, Osaka 560, Japan

H. Sakai

Research Center for Nuclear Physics, Osaka University, Suita, Osaka 565, Japan

(Received 21 July 1982; revised manuscript received 4 January 1983)

Pre-equilibrium and equilibrium deexcitation processes for $(\alpha, xn\gamma)$ reactions induced by 50—120 MeV α particles were studied. Reaction channels were identified by measuring rotational γ rays characteristic of the reaction residues. The branching of the reaction channels gave neutron multiplicity distributions. Features characteristic of the pre-equilibrium process were seen in the reaction channels with small neutron multiplicity x. An exciton model calculation code was developed so as to incorporate both multiparticle emission at the fast pre-equilibrium stage and multiparticle evaporation at the slow equilibrium stage. The calculation reproduced the neutron multiplicity distributions in the whole range of $E_\alpha = 50-120$ MeV. The pre-equilibrium fractions and the entry lines from the pre-equilibrium stage to the equilibrium one were deduced. The pre-equilibrium fractions were found to be approximately 40—60%, being rather independent of the individual reaction channel. The entry lines slowly increase from 25 to 35 MeV with increasing projectile energy.

I. INTRODUCTION

Mechanisms of fusionlike (particle, $xnyp\gamma$) reactions induced by medium energy projectiles with several tens of MeV per nucleon are of current interest because of the competition between pre-equilibrium (PEQ) and equilibrium (EQ) deexcitation processes.[1] The (particle, $xn, yp\gamma$) reactions induced by projectiles below about 10 MeV per nucleon have been well described in terms of a statistical process through compound nucleus formation, where the nucleus deexcites by evaporating low energy particles at the EQ phase. As the projectile energy increases beyond around 20—30 MeV per nucleon, fast particle emission at the first few doorways to the PEQ stage becomes significant because the particle escape width at this stage becomes large.[2] Several models have been proposed to deal with the deexcitation process of the highly excited nucleus produced by nuclear reactions. They are the intranuclear cascade model (INC),[3] the quasifree scattering model (QFS),[4] and the PEQ exciton model.[5-8] These models have been used to describe various experimental data. In the case of the fusionlike (particle, $xnyp\gamma$) reactions in the medium energy range, the exciton model has been considered to be the most suitable description. In this model, interactions between nucleons of the projectile and those of the target nucleus produce excited particles (p) and holes, (h), namely excitons. These excitons collide with nucleons in the nucleus. This process gives rise to additional exciton spreading. Some of the energetic particles in excitons may escape out of the nucleus in the course of the exciton spreading. The average exciton energy de-

creases due to the emissions of these energetic exciton particles. The spreading process results in an increase of the exciton number $(n = p + h)$ and a decrease of their average kinetic energy. Hence, particle escape becomes less likely and the nucleus becomes thermally equilibrated; subsequently the nucleus cools down to the entry point of the reaction residues by evaporating slow particles (mostly neutrons in the cases of medium and heavy nuclei). Finally the nucleus deexcites down to the ground state by emitting γ rays.

It is preferable to measure exclusive neutron spectra following (particle, $xnyp\gamma$) reactions as a function of the neutron multiplicity x, because the effects of the PEQ process are then most apparent. Previously, Ejiri et al.[2] made such exclusive measurements in a detailed study of the ^{165}Ho$(p, xn\gamma)$ reaction at $E_p = 60$ MeV, and found the evidence for PEQ emission of neutrons. The (particle, $xn\gamma$) reaction mechanism has also been studied by measuring singles γ-ray spectra and the γ-ray multiplicity.[9,10] Observation of the spin alignment of the yrast levels populated by the (particle, xn) reaction supports the PEQ neutron deexcitation process.[11] Their results suggest that a considerable fraction of the input angular momentum is carried away by the PEQ neutrons. The deexcitation process following the reactions induced by heavy ions has also been investigated by several investigators.[12-16] They found PEQ properties in their data for incident energies of 12—15 MeV per nucleon.

The present study was made to observe the behavior of the $(\alpha, xn\gamma)$ reactions as the incident energy is decreased from above the Fermi energy to below the Fermi energy.

In this region, the PEQ and EQ processes are thought to coexist. We studied the reaction process by measuring γ rays of the reaction residue as in previous work.[2] Rare earth nuclei of ^{162,164}Dy and ^{174,176}Yb were chosen as targets because the rotational levels and other low-lying levels in the residual isotopes are well known. The discrete γ rays from the rotational levels, which are characteristic of the residual nuclei (reaction channels), were used to determine the cross sections of the various channels. They give the neutron multiplicity distributions. The observed distributions were analyzed in terms of the exciton model with a multiparticle emission process.

II. EXPERIMENTAL PROCEDURE AND RESULTS

Incident α particles in an energy range from 50 to 120 MeV were provided by the 230 cm AVF cyclotron at the RCNP, Osaka University. Enriched ^{162,164}Dy and ^{174,176}Yb targets were prepared by depositing the oxide powder on thin Mylar films of 30 μm in thickness. Table I lists the targets and energies of the incident α particles used in the present experiment.

The neutron multiplicity distribution $\sigma(x)$ for the $_{Z}^{A}X(\alpha,\mathrm{xn}\,\gamma)_{Z+2}^{B}Y$ is given by the mass distribution of the residual isotope $_{Z+2}^{B}Y$, where the mass B is $A+4-x$. The cross section for the isotope $_{Z+2}^{B}Y$ is obtained from the yield of γ rays characteristic of the reaction residue $_{Z+2}^{B}Y$.[2] Because of the large number of the open reaction channels at the present projectile energy, the γ-ray spectrum is very complicated. In order to resolve discrete γ rays corresponding to individual reaction channels, we used a 1.5 cm^3 pure Ge detector (LEPS) with an energy resolution of $\Delta E = 1$ keV for 511 keV γ rays. The detector was placed at 125°, where $P_2(\cos\theta)=0$, with respect to the beam axis. The γ-ray yield at this angle gives approximately the total cross section because the higher order term $A_2 P_2(\cos\theta)$ is at most a few percent. The counting rate was always kept below 700 counts per sec in order to avoid uncertainty due to the dead time correction.

Total cross sections for the even-even isotopes are estimated from the γ-ray yields of the yrast cascade $6^+ \rightarrow 4^+ \rightarrow 2^+ \rightarrow 0^+$. The yrast γ-ray yields give the population of the yrast levels 6^+, 4^+, 2^+, 0^+ and the extrapolation to the 0^+ population which gives the yields of the residual nuclei. Cross sections for the odd mass isotopes are estimated from the γ-ray yields of the yrast

$$21/2^+ \rightarrow 17/2^+ \rightarrow 13/2^+$$

transitions and yrare

$$19/2^+ \rightarrow 15/2^+ \rightarrow 11/2^+$$

transitions. Here we have corrected for contributions from other possible γ rays by referring to relative γ intensities observed in other inbeam-γ experiments.[17] The γ-ray yields have been corrected for the conversion electrons.

The neutron multiplicity distributions for the ^{162,164}Dy and ^{174,176}Yb$(\alpha,\mathrm{xn}\,\gamma)$ reactions at $E_\alpha = 50$, 70, 90, 70, and 120 MeV are presented in Fig. 1. The cross sections for small x are much larger than the prediction of the compound nucleus model (the dotted lines in Fig. 1). This feature is taken to be characteristic of the PEQ process. This feature gets more pronounced as the projectile energy gets higher. Since the Q values for the $(\alpha,\mathrm{xn}\,\gamma)$ reactions are approximately given by $Q(x) = -8x$ (MeV), the average neutron energy is expressed as

$$\bar{E}_n = (E_\alpha - 8x - E_\gamma)/x$$
$$= (E_\alpha - E_\gamma)/x - 8 \text{ (MeV)}, \tag{1}$$

where E_γ is the entry point of the γ decay. Thus, reactions with small neutron multiplicity x correspond to reactions with large kinetic energy of the deexciting neutrons.

III. ANALYSIS AND COMPARISON WITH EXPERIMENTAL RESULTS

A. Cascade calculation of the PEQ-EQ process

The neutron multiplicity distribution was analyzed in terms of the exciton model for a multiparticle emission process. The decay rates of the exciton particles are key parameters in the exciton model calculation. We used values reported in previous works.[18-21] A Monte Carlo method developed by Dostrovsky et al.[22] has been extended to the present PEQ-EQ process. This method is similar to that employed by Gadioli et al.[23] to calculate the integral spectra of decay particles and the excitation functions.

At the beginning of the calculation we numerically evaluated the escape rates for all relevant particles and for all sets of (p,h) values. In order to follow the cascade process, the decay sequence was determined by use of random numbers. The calculation of the PEQ cascade continues until $\Gamma_{\bar{n}}^{+} = \Gamma_{\bar{n}}^{-}$, where $\Gamma_{\bar{n}}^{+}$ and $\Gamma_{\bar{n}}^{-}$ are the spreading widths of the increasing and decreasing process of excitons, respectively, and $\bar{n}$ denotes the mean value of the exciton number at this condition. At this point the mean exciton number $\bar{n}$ is approximately given by $\bar{n} = \sqrt{1.5gE}$, where E is the excitation energy and g is the single particle level density. Subsequently, the PEQ cascade transits to the EQ one. The EQ process was calculated by the same method as that in Ref. 22. The EQ cascade calculation proceeds until the excitation energy becomes lower than the neutron threshold energy. These PEQ-EQ deexcitation calculations are repeated many times to obtain good statistics by the Monte Carlo process. In what follows, we describe the evaluation of the energy distribution for the escaping particles, and of the spreading and escape widths for a given excitation energy and exciton number.

The escape probability $W_b^m(\epsilon)$ for a particle b with the kinetic energy at the m exciton state of the PEQ process can be expressed as [19]

TABLE I. Targets, their isotopic enrichments and their thicknesses, and incident energies of α particles.

Target	Target isotopic enrichment (%)	Thickness (mg/cm^2)	Projectile energy (MeV)
^{162}Dy	95.0	4.0	70, 90, 120
^{164}Dy	98.4	3.3	50, 90, 120
^{174}Yb	95.8	4.5	70, 90, 120
^{176}Yb	96.4	5.0	50, 70, 90, 120
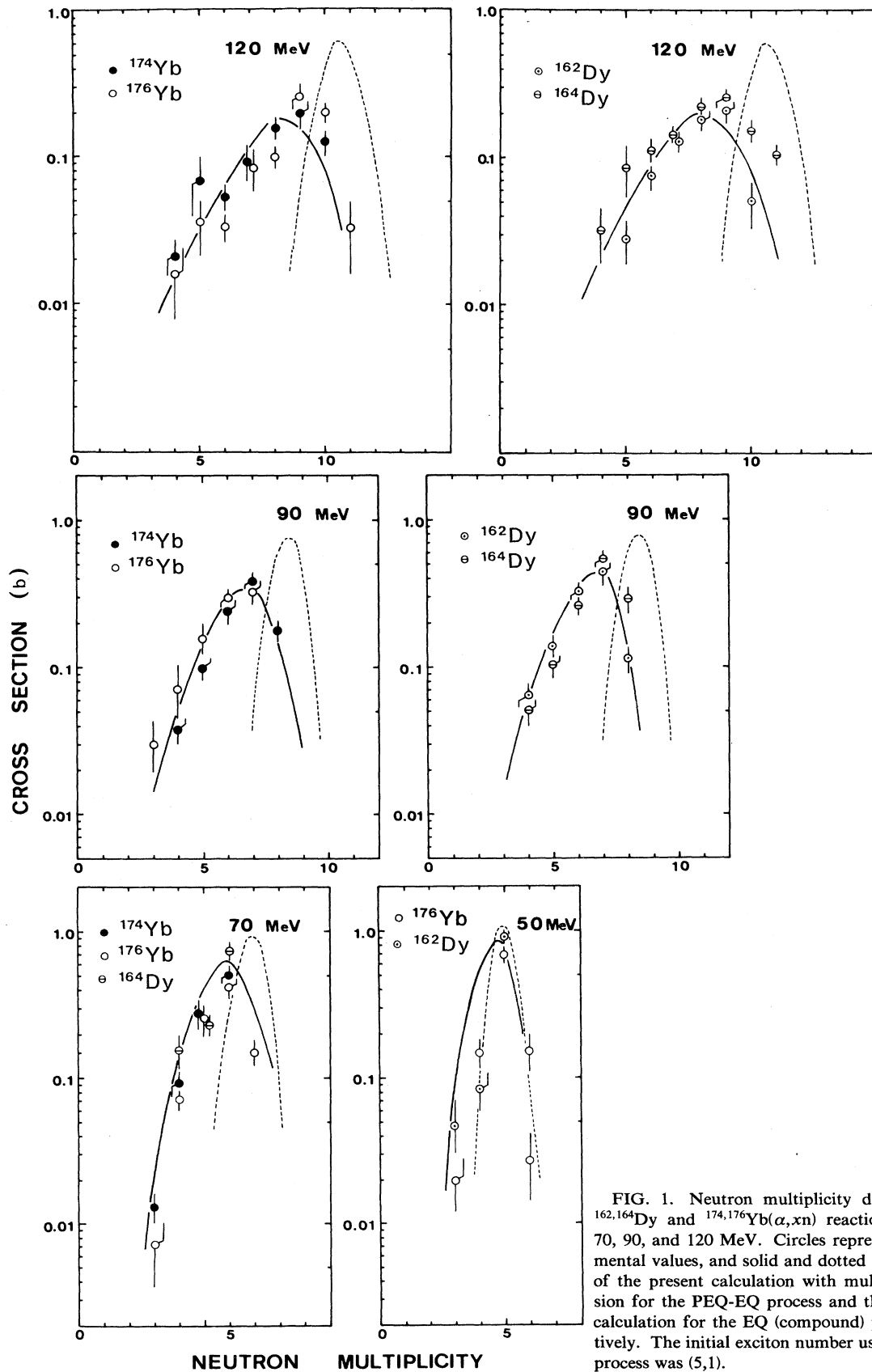
FIG. 1. Neutron multiplicity distributions for ^{162,164}Dy and ^{174,176}Yb(α,xn) reactions at $E_\alpha = 50$, 70, 90, and 120 MeV. Circles represent the experimental values, and solid and dotted lines are results of the present calculation with multiparticle emission for the PEQ-EQ process and the conventional calculation for the EQ (compound) process, respectively. The initial exciton number used for the PEQ process was (5,1).

$$W_b^m(\epsilon) = \frac{2s_b + 1}{\pi^2 \hbar^3} \mu_b \epsilon \sigma_b(\epsilon) R_b(p,h) P_b!$$

$$\times \frac{\rho(E - \epsilon - B_b, p - p_b, h)}{\rho(E, p, h)}, \tag{2}$$

where s_b, μ_b, B_b, and p_b are, respectively, the spin, reduced mass, binding energy, and nucleon number for the escaping particle b. The level densities $\rho(E,p,h)$ and $\rho(E - \epsilon - B_b, p - p_b, h)$ denote the initial and final level density, respectively. It can be written as[24]

$$\rho(E,p,h) = g \frac{(gE - A_{p,h})^{p+h-1}}{p!\,h!\,(p+h)!}, \tag{3}$$

where g is the single particle state density in the equal spacing model, which is related to the level density parameter a by $g = 6a/\pi^2$. The factor $A_{p,h}$ is a correction term for the first order effect of the Pauli-exclusion principle, and is simply given by

$$A_{p,h} = (p^2 + h^2 + p - 3h) .$$

The extra two parameters of $R_b(p,h)$ and $P_b!$ are empirical adjustment factors introduced by Cline.[19] The mean absorption cross section $\sigma_b(\epsilon)$ is assumed to be

$$\sigma_n(\epsilon) = \pi R^2 \tag{4}$$

for a neutron and

$$\sigma_b(\epsilon) = 0 \quad \epsilon \le V_C$$

$$= \pi R^2(1 - V_C/\epsilon) \quad \epsilon > V_C ,$$

for charged particles, where R is the nuclear radius. The Coulomb barrier height V_C is obtained as

$$V_C = 1.44zZ/[r_0(1 + A^{1/3})] \text{ (MeV) .} \tag{5}$$

The escape width is defined as

$$\Gamma_m = \hbar \int_0^{E - B_b} W_b^m(\epsilon) d\epsilon . \tag{6}$$

The transition rates for the spreading process can be estimated from the first-order time dependent perturbation theory.[19,21] The spreading width Γ_m^+ for the internuclear collision with $\Delta p = \Delta h = +1$ and the width Γ_m^- for that with $\Delta p = \Delta h = -1$ are written as

$$\Gamma_m^+(E,p,h) = \pi |\overline{M}|^2 \frac{g}{p+h+1}(gE - C_{p+1,h+1})^2 , \tag{7}$$
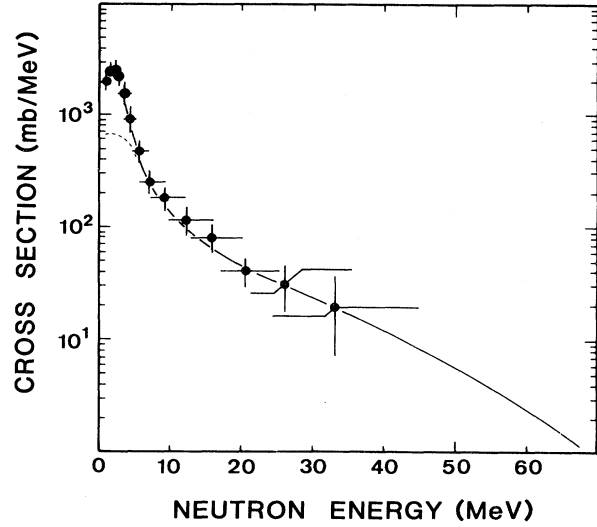
FIG. 2. Calculated energy spectra of the neutrons following the ^{165}Ho(α,xn) reaction at $E_\alpha = 109$ MeV, where dotted lines and closed circles represent the contributions of the pre-equilibrium process and the experimental value (Ref. 25), respectively.

and

$$\Gamma_m^-(E,p,h) = \pi |\overline{M}|^2 gph(p+h-2) , \tag{8}$$

where

$$C_{p,h} = (p^2 + h^2)/2$$

is the correction due to the Pauli principle and $|\overline{M}|^2$ is the average square of the transition matrix element for the present neutron emission through the PEQ cascade process. The value of $|\overline{M}|^2$ has been approximated by an empirical formula developed by Cline,[19] where it is given as

$$|\overline{M}|^2 = kA^{-3}E^{-1} , \tag{9}$$

with $k = 1450$ MeV^3. In the present analysis, we take for simplicity the same form to see how the present data are reproduced by an effective matrix element.

TABLE II. PEQ fraction $f_p(\%) = 100 n_p/(n_p + n_e)$ in the calculated neutron cross section of ^{164}Dy$(\alpha x n \gamma)$ reactions, where n_p and n_e are the number of neutrons emitted at the PEQ and EQ phase, respectively.

Energy (MeV)	first emission	second emission	third emission	fourth emission	fifth emission	sixth emission	seventh emission
50	100	80	20	4			
70	100	94	55	40	2		
90	100	97	73	63	20	5	
120	100	99	85	75	44	30	2
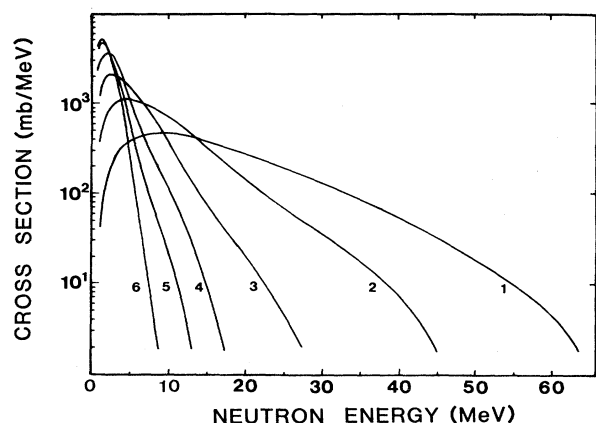
FIG. 3. Calculated energy spectra of the first, second, third, fourth, fifth, and sixth neutrons following ^{164}Dy(α,xn) reactions at $E_\alpha = 90$ MeV. The initial exciton number used in the calculation was (5,1).

B. Comparison with experiment

The exciton model calculation has been carried out by starting with the initial exciton number $(p,h) = (5,1)$, as in the case of previous exciton model calculations[18] for α particles. The idea is that the first doorway stage for the $(\alpha, x n \gamma)$ reaction is formed by the interaction of an α projectile with a nucleon in a nucleus, resulting in the breakup of the α particle into 4-exciton particles and a particle-hole exciton. The general trend of neutron multiplicities has been reproduced with $k = 730$ MeV.[3] The experimental values of the neutron multiplicity distributions are compared with the calculated values in Fig. 1. The calculated multiplicity distributions for the 120 MeV α projectile, however, underestimate the observed values at the large neutron multiplicity (large x), as shown in Fig. 1. This is probably due to an overestimation of the PEQ process. The treatment used in the lower excitation region (< 90 MeV) may not be suitable for such a high excitation region.

IV. DISCUSSION

The conventional exciton model deals with only the first emission from the PEQ stage. This approach can be justified when the PEQ fraction is small in the second emission. Such a situation can be satisfied in two cases. Firstly, the initial excitation energy is lower than about 30 MeV and only one particle can be emitted at the PEQ. Secondly, only the high energy component of the emitted particles is concerned. Note that the 5—10 MeV neutrons can still be emitted at the PEQ stage of medium heavy nuclei, in contrast to charged particles which are inhibited by the Coulomb barrier. In order to extend the exciton model to more energetic reactions and multineutron emissions, the multiparticle emission process at the PEQ stage has to be considered. The neutron energy spectrum calculated by the multiparticle emission method is illustrated in Fig. 2, where the experimental points have been obtained by means of a time-of-flight method.[25] The calculated PEQ contribution in the low energy part can be seen to be large. The total PEQ fraction is 54%, where the PEQ fraction is defined as the ratio of the number of the PEQ neutrons which are emitted before the condition $\Gamma_m^+ = \Gamma_m^-$ and the total neutron number. It increases from 50% to 64% in the neutron energy distributions with increasing initial excitation energy from 50 to 120 MeV (see Table II). The maximum error at each excitation is about 10%, which comes from the discrepancy between the experimental neutron multiplicity distribution and the calculated one. With the same initial condition, the neutron energy distributions from the first to sixth neutron emissions are shown in Fig. 3. The PEQ fractions decrease from 100% to 2%. As shown in Table II, the second and third emissions have significant PEQ fractions, which increase with the increase of the excitation energy. The PEQ fraction of each reaction channel is presented in Table III. They distribute between 40% and 65%. These PEQ fractions are approximately constant in the same number of the neutron multiplicity, and the dependence of the initial excitation energy is relatively small.

The mean excitation energy of the entry point from the PEQ stage to the EQ one can be estimated as

TABLE III. PEQ fractions $f_p^x(\%)$ of individual reaction channels in the calculated neutron cross section in ^{164}Dy$(\alpha, x n \gamma)$ reactions.

Energy (MeV)				
x	50	70	90	120
3	40			
4	45	44	45	
5	48	50	50	49
6	57	57	55	52
7		57	60	60
8			64	65
9			60	64
10				65
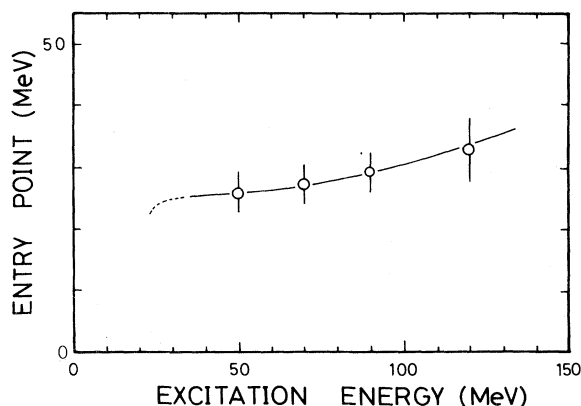
FIG. 4. Estimated entry line from the PEQ process to the EQ one for the ^{164}Dy$(\alpha x n)$ reaction with exciton number (5,1).
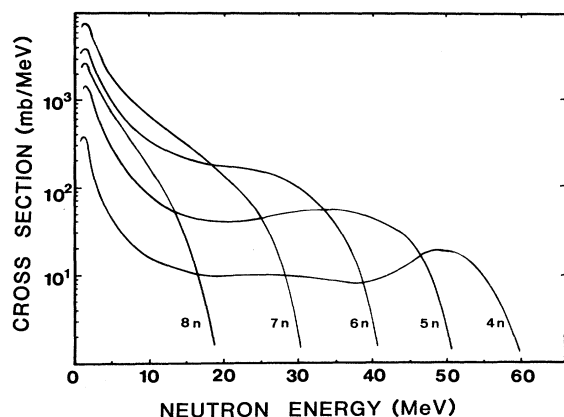
FIG. 5. Calculated neutron energy spectra of individual reaction channels. The initial nucleus, excitation energy, and exciton number are ^{168}Er, 90 MeV, and (5,1), respectively.

$$E \approx x f_e 2kT_e + E_\gamma , \tag{10}$$

where x is the neutron multiplicity, f_e is the EQ fraction of the

$$2kT_e \approx \tfrac{4}{3}\sqrt{E_x/a}$$

is the mean energy of neutrons emitted at the EQ stage. The estimated entry points are illustrated in Fig. 4. The excitation energy of the entry point is nearly constant over a wide range of excitation energies. Typical neutron energy spectra of the individual reaction channels are shown in Fig. 5, where the initial exciton energy and the excitation number are 90 MeV and (5,1), respectively. The neutron energy distributions, especially in the $4n$ and $5n$ channels, extend with large intensity up to 40—50 MeV. So far no measurement has been made of the neutron energy spectra for individual reaction channels.

V. SUMMARY

The $(\alpha, xn\gamma)$ reactions on targets of ^{162,164}Dy and ^{174,176}Yb were studied by measuring discrete γ rays. The experimentally obtained neutron multiplicity distributions were compared with an exciton model for multiparticle emission. The results are summarized as follows:

(1) Experimental evidence for the PEQ process in the form of cross sections much larger than EQ model predictions were obtained in the reaction channels with small neutron multiplicity x. Furthermore, the average neutron energy $\bar{E}_n \gg 2kT_e$.

(2) The exciton model calculation for the multiparticle emission process was applied for the present analysis. The neutron multiplicity distributions were well reproduced with the initial exciton number of (5,1) for the present α-particle induced reactions. Comparing the experimental results with the calculations, the PEQ fractions and the entry point to the EQ stage were deduced. These quantities are roughly constant for various reaction channels in a wide range of the initial excitation energy.

(3) Effective collision probabilities in the excited nuclei were estimated from the comparisons between the experiments and the calculations. They agree with the expectations of other models and calculations for the first doorway state.

*Present address: Department of Physics, College of General Education, Tohoku University, Kawauchi, Sendai 980, Japan.

[1] H. Feshbach, Rev. Mod. Phys. 46, 1 (1974).

[2] H. Ejiri, T. Shibata, T. Itahashi, Y. Nagai, H. Sakai, S. Nakayama, T. Kishimoto, K. Maeda, and H. Hoshi, J. Phys. Soc. Jpn. Suppl. 44, 655 (1978); H. Ejiri et al., Nucl. Phys. A305, 167 (1978); H. Sakai et al., Phys. Rev. C 22, 1002 (1980).

[3] M. L. Goldberger, Phys. Rev. 74, 1289 (1948); K. Chen, G. Friedlander, G. D. Harp, and J. M. Miller, Phys. Rev. C 4, 2234 (1971).

[4] A. Mignerey, M. Blann, and W. Scobel, Nucl. Phys. A273, 125 (1976).

[5] J. J. Griffin, Phys. Rev. Lett. 17, 478 (1966).

[6] M. Blann, Annu. Rev. Nucl. Sci. 25, 123 (1975).

[7] D. Agassi, H. A. Weidenmüller, and G. Mantzouranis, Phys. Rep. 22, 145 (1975).

[8] E. Gadioli, E. Gadioli-Erba, and P. G. Sona, Nucl. Phys. A217, 570 (1973).

[9] W. J. Ockels, M. J. A. de Voigt, and Z. Sujkcuski, Phys. Lett.

48B, 4 (1978); M. J. A. de Voigt et al., Nucl. Phys. A323, 317 (1979).

[10] J. R. Beene, M. L. Halbert, D. C. Hensley, R. A. Dayras, K. G. Young, D. G. Sarantites, and J. H. Barker, Phys. Rev. C 23, 2463 (1981).

[11] T. Kishimoto, M. Sasao, H. Suzuki, H. Sakai, and H. Ejiri, Nucl. Phys. A337, 493 (1980); Y. Nagai, T. Shibata, H. Sakai, T. Kishimoto, and H. Ejiri, J. Phys. Soc. Jpn. 46, 1025 (1979).

[12] A. Gavron, J. R. Beene, R. L. Ferguson, F. E. Obenshain, F. Plasil, G. R. Young, G. A. Petitt, K. G. Young, M. Jaaskelanen, D. G. Sarantites, and C. F. Maguire, Phys. Rev. C 24, 2048 (1981).

[13] H. Yamada, D. R. Zolnowski, S. E. Cala, A. C. Kahler, J. Pierce, and T. T. Sugihara, Phys. Rev. Lett. 43, 605 (1979).

[14] H. Utsunomiya, T. Nomura, T. Inamura, T. Sugitate, and T. Motobayashi, Nucl. Phys. A334, 127 (1980).

[15] D. G. Sarantites, L. Westerberg, R. A. Dayras, M. L. Halbert, D. C. Hansley, and J. H. Barker, Phys. Rev. C 17, 601 (1978).

[16]L. Westerberg, D. G. Sarantites, D. C. Hensley, R. A. Dayras, M. L. Halbert, and J. H. Barker, Phys. Rev. C 18, 796 (1978).

[17]H. Ryde, S. A. Hjorth, D. Barneoud, A. Johnson, G. B. Hargemann, and B. Herskind, Nucl. Phys. A207, 513 (1973); S. A. Hjorth *et al., ibid.* A144, 513 (1970); A. Johnson, H. Ryde, and J. P. Torres, *ibid.* A175, 167 (1971); K. Krien *et al., ibid.* A209, 572 (1973); W. Andrejtscheff *et al., ibid.* A220, 438 (1974); E. Gosse, F. S. Stephans, and R. M. Diamond, Phys. Rev. Lett. 31, 840 (1973); M. V. Banaschik *et al.,* Nucl. Phys. A222, 459 (1974); W. Andrescheff *et al., ibid.* A225, 300 (1974).

[18]J. R. Wu, C. C. Chang, and H. D. Hogan, Phys. Rev. C 19, 659 (1979); 19, 698 (1979).

[19]C. K. Cline, Nucl. Phys. A192, 353 (1972); A193, 417 (1972).

[20]S. Yoshida, Proceedings of the IPCR Symposium, 1977, IPCR Cyclotron Report, Suppl. 6, p. 359.

[21]P. Oblozinski, I. Ribanski, and E. Betak, Nucl. Phys. A226, 347 (1974); C. Kalbach, Z. Phys. A 283, 401 (1977).

[22]I. Dostrovsky, Z. Frankel, and L. Winsberg, Phys. Rev. 118, 781 (1960).

[23]E. Gadioli, E. Gadioli-Erba, and J. J. Hogan, Phys. Rev. C 16, 1404 (1977).

[24]F. C. Williams, Jr., Nucl. Phys. A166, 231 (1971).

[25]K. Maeda, thesis, Osaka University, 1980.